NIH Public Access
Author Manuscript
J Comp Neurol. Author manuscript; available in PMC 2011 October 15.

Published in final edited form as:
J Comp Neurol. 2010 October 15; 518(20): 4213–4225. doi:10.1002/cne.22449.

Neuregulin-1 at Synapses on Phrenic Motoneurons

Amine N. Issa[1], **Wen-Zhi Zhan**[1], **Gary C. Sieck**[1,2], and **Carlos B. Mantilla**[1,2,*]

[1]Department of Physiology & Biomedical Engineering, College of Medicine, Mayo Clinic Rochester, MN 55905

[2]Department of Anesthesiology College of Medicine, Mayo Clinic Rochester, MN 55905

Abstract

The neuregulin (NRG) family of trophic factors is present in the central and peripheral nervous systems and participates in the survival, proliferation and differentiation of many different cell types including motoneurons. NRG1 was first characterized by its role in the formation of the neuromuscular junction, and recently it was shown to play a crucial role in modulating glutamatergic and cholinergic transmission in the central nervous system of adult rats. However, little is known about NRG1's role in adult motor systems. Motoneurons receive dense glutamatergic and cholinergic input. We hypothesized that NRG1 is present at synapses on phrenic motoneurons. Confocal microscopy and 3D reconstruction techniques were used to determine the distribution of NRG1 and its co-localization with these different neurotransmitter systems. We found that NRG1 puncta are present around retrogradely-labeled motoneurons, and are distributed predominantly at motoneuron somata and primary dendrites. NRG1 is exclusively present at synaptic sites (identified using the presynaptic marker synaptophysin), comprising ~30% of all synapses at phrenic motoneurons. Overall, NRG1-immunoreactivity is found predominantly at cholinergic synapses (75 ± 14% co-localize with the vesicular acetylcholine transporter VAChT). Nearly all (99 ± 1%) VAChT-immunoreactive synapses expressed NRG1. NRG1 also is present at a subset of glutamatergic synapses expressing the vesicular glutamate transporter (VGLUT) type 2 (~6%) and not those expressing VGLUT type 1. Overall, 26 ± 6% of NRG1 synapses are VGLUT2 immunoreactive. These findings provide the first evidence suggesting that NRG1 may modulate synaptic activity in adult motor systems.

Keywords

NRG1; VAChT; Cholinergic; Glutamatergic; VGLUT; Synaptophysin

INTRODUCTION

Neuregulins (NRG) are members of the larger epidermal growth factor (EGF) family of trophic factors that activate receptor tyrosine kinases of the ErbB family (Trinidad et al., 2000; Zhu et al., 1995). There are four known NRG genes (NRG 1–4), each with multiple isoforms that display significant variability in their tissue expression (Buonanno and Fischbach, 2001; Falls, 2003). Several components of the neuromuscular system express NRG genes and their receptors. Spinal motoneurons express NRG1 and ErbB receptor mRNA (Lindholm et al., 2002; Ricart et al., 2006). Schwann cells and muscle fibers express NRG1 (mRNA and protein) as well as ErbB receptors at the neuromuscular junction (Jo et al., 1995; Kerber et al., 2003; Zhu et al., 1995).

*Carlos B. Mantilla, M.D., Ph.D. Joseph 4W-184F, SMH 200 First St SW Rochester, MN 55905 Phone: 507-255-7481 Fax: 507-255-7300 mantilla.carlos@mayo.edu.

NIH-PA Author Manuscript
NIH-PA Author Manuscript
NIH-PA Author Manuscript

NIH-PA Author Manuscript

NIH-PA Author Manuscript

NIH-PA Author Manuscript

A role for NRG1 in neuromotor control during embryonic development was first described at the neuromuscular junction, where NRG1 regulates acetylcholine (ACh) receptor expression (Jo et al., 1995; Loeb et al., 2002; Sandrock et al., 1997; Zhu et al., 1995). In addition, it was shown that early motoneuron survival depends on NRG1, albeit through a complex interplay with other trophic factors including neurotrophins (Ricart et al., 2006). In the cerebellum, NRG1 controls the expression of glutamatergic N-methyl D-aspartate (NMDA) receptors (Ozaki et al., 1997; Ozaki et al., 2000) and at hippocampal interneurons, it modulates both glutamatergic and cholinergic neurotransmission (Chang and Fischbach, 2006; Li et al., 2007; Zhong et al., 2008). Multiple studies have reported widespread distribution of both glutamatergic and cholinergic synaptic inputs at motoneurons (Bae et al., 1999; Herzog et al., 2004; Shigenaga et al., 2005), including phrenic motoneurons (McCrimmon et al., 1989; Murphy et al., 1996; Tai and Goshgarian, 1996; Zhan et al., 1989). However, there is very limited information regarding NRG1 in adult motor systems. In the present study, we explored the hypothesis that NRG1 is present at synaptic sites on adult PhrMn using confocal microscopy and 3D reconstruction analyses. We report here that NRG1 is present at synapses on PhrMn, predominantly at cholinergic synapses present on motoneuron somata and primary dendrites, with less abundant expression at glutamatergic synapses. The characterization of NRG1 distribution and its association with specific neurotransmitter systems are important first steps in elucidating the possible role of neuregulin in the adult neuromuscular system.

METHODS

Animals

A total of 14 adult male Sprague-Dawley rats (Colony 236, Harlan, Indianapolis, IN; 280 – 300 g initial body weight) were used in this study. All procedures were approved by the Institutional Animal Care and Use Committee at Mayo Clinic and conducted in strict accordance with the National Institutes of Health Guide for the Care and Use of Laboratory Animals (NIH Publications No.80-23 revised 1996).

Phrenic Motoneuron Labeling and Tissue Processing

An intramuscular injection was performed to retrogradely label PhrMn, in accordance with previously published techniques (Kinkead et al., 1998; Mantilla et al., 2009; Prakash et al., 2000). Rats were anesthetized with a mixture of ketamine (90 mg/kg) and xylazine (10 mg/kg) and, using a laparotomy to expose the diaphragm muscle, 2–3 μl of cholera toxin B subunit (0.2% in distilled water; List Biological Laboratories) were injected into the sternal and costal portions of the diaphragm at each of 6–8 sites. In some cases, Alexa 488-conjugated cholera toxin B (Invitrogen Corp., Carlsbad, CA) was used (see section on Immunohistochemistry below). After two to three days, rats were anesthetized with the same anesthetic mixture of ketamine and xylazine and transcardially perfused with 4% paraformaldehyde in 0.1M phosphate buffer solution (PBS; pH 7.6). The cervical spinal cord was removed and post-fixed in 4% paraformaldehyde in 0.1 M PBS overnight. The tissue was then transferred to 24% sucrose in 0.1M PBS for 24–72 hours before cryo-sectioning. Using a Leica 2800E Frigocut Microtome Cryostat (Leica Microsystems, Wetzlar, Germany), 50 or 100 μm thick longitudinal or transverse sections were obtained. The sections were stored in 0.05M Tris-buffered saline (TBS: Tris; 0.15M NaCl; pH 7.5) until ready for use.

Immunohistochemistry

The immunohistochemical procedures used were based on previously reported techniques (Kinkead et al., 1998; Prakash et al., 2000; Zhan et al., 2000). Briefly, spinal cord sections were blocked for one hour in 5–10% normal donkey serum in TBS containing 0.3% Triton

NIH-PA Author Manuscript

NIH-PA Author Manuscript

NIH-PA Author Manuscript

X-100 (TBS-Tx), followed by incubation overnight (16–24 hours) with the appropriate primary antibodies (see Table 1 and Primary Antibody Characterization section below) in 5% normal donkey serum TBS-Tx. After being washed three times in TBS (10–15 minutes each), sections were incubated with FITC-, Cy3- and Cy5-labeled donkey secondary antibodies (IgG; Jackson ImmunoResearch Laboratories, Inc. West Grove, PA) for two to four hours. FITC-conjugated anti-goat antibody was used for detection of anti-cholera toxin B in all cases, except for those where PhrMn were labeled directly with Alexa 488-conjugated cholera toxin B. A Cy3-conjugated anti-rabbit antibody was used for detection of NRG1. A Cy5-conjugated anti-mouse antibody was used for detection of anti-synaptophysin, VGLUT1 and VGLUT2. VAChT was detected using a Cy5-conjugated anti-goat antibody in sections where PhrMn were directly labeled with Alexa 488 conjugate. Tissue sections were then washed three times in TBS before being mounted, air dried and dehydrated in graded alcohol concentrations of 70%, 95%, and 100% (each for 5–15 minutes). Excess alcohol was removed by placing the slide in xylene for 5–15 minutes. Sections were mounted using a DPX histochemical mounting solution (Fluka Chemical Corp Milwaukee, WI) and cover-slipped. For all primary/secondary antibody pairs, additional studies not including the primary antibody (blank) or alternately using Cy3- or Cy5-conjugated secondary antibodies were conducted to confirm the specificity of immunostaining. Blank sections were processed in parallel for all immunohistochemical reactions and animals.

Primary Antibody Characterization

A complete list of primary antibodies used and the immunogens is provided in Table 1. The anti-cholera toxin B antibody used to identify retrogradely labeled PhrMn was raised against a highly purified form of this toxin derived from Vibrio cholera (Mekalanos et al., 1978;Rappaport et al., 1974). The specificity of retrograde-labeling was confirmed by the absence of staining in tissues of rats injected with vehicle (no toxin), as previously reported (Mantilla et al., 2009). The staining pattern in the spinal cord of toxin injected rats revealed immunoreactivity that was identical with previous descriptions (Kinkead et al., 1998;Mantilla et al., 2009;Prakash et al., 2000;Prakash et al., 1993;1994).

The NRG1 antibody (anti-neureguilin-1α/β1/2) was chosen to identify all NRG1 isoforms. We confirmed that this antibody specifically recognizes a single protein band at ~50 kD in immunophoretically-separated rat spinal cord tissue (Fig. 1), in agreement with the manufacturer's technical information. All immunostaining in rat spinal cord was abolished when 0.5 ml of the diluted primary antibody was preincubated with 8 μg of the immunizing peptide (Fig. 1).

For identification of synaptic sites on PhrMn, we selected an anti-synaptophysin antibody that specifically recognizes a region between amino acids 269 and 289 (Knaus and Betz, 1990) in the cytoplasmic domain of this integral membrane glycoprotein (~40 kD) (Wiedenmann and Franke, 1985). The antiserum stains a single band of 38 kD molecular weight on Western blot (manufacturer's technical information). The punctate immunoreactivity pattern observed was identical to previous reports in rat spinal tissue (Hellstrom et al., 1999; Herzog et al., 2004).

For identification of cholinergic synapses around PhrMn, we used an antibody to vesicular acetylcholine transporter (VAChT). The antiserum stains a single band of 55 kD molecular weight on Western blot (manufacturer's technical information). The staining pattern identified by this antibody is identical to previous reports of cholinergic boutons distributed proximally around motoneurons in the rat spinal cord (Hellstrom et al., 1999; Wilson et al., 2004)

NIH-PA Author Manuscript

NIH-PA Author Manuscript

NIH-PA Author Manuscript

Antibodies to VGLUT1 and VGLUT2 were used to identify glutamatergic synapses around PhrMn. These antisera stain a single band (VGLUT1: 60 kD; VGLUT2: 56 kD molecular weight) on Western blot (manufacturers' technical information). Staining of rat spinal tissue produced a pattern of VGLUT1 and VGLUT2 immunoreactivity around motoneurons identical to previous descriptions (Alvarez et al., 2004; Herzog et al., 2004)

Confocal Imaging

Spinal cord sections were imaged using an Olympus Fluoview 300 laser scanning confocal microscope (Olympus America Inc., Melville, NY, USA) mounted on an upright Olympus BX50WI microscope equipped with argon (488 nm), green HeNe (543 nm) and red HeNe (633 nm) lasers. Three-dimensional imaging techniques have been previously reported (Prakash et al., 2000; Prakash et al., 1993; 1994; Sieck et al., 1999; Zhan et al., 2000). All images were acquired at 12-bit resolution in an array of 1024×768 pixels. For analyses of NRG1 distribution, labeled samples were imaged using 40× oil immersion lens (NA 1.35) with a step size of 1 μm. Hence, each voxel corresponded to 0.5 × 0.5 × 1 μm. For analyses of NRG1 co-localization with specific synaptic markers, labeled samples were imaged using a 60× oil immersion lens (NA 1.4) with a step size of 0.75 μm (voxel dimensions: 0.33 × 0.33 × 0.75 μm). Simultaneous two- or three-color imaging was performed using a dichroic mirror beam splitter that allows transmission of 555–615 nm (reflects 480–555 and 615–800 nm) and appropriate band pass emission filters (495–535 nm, 575–630 nm and 645 nm long pass for FITC/Alexa 488, Cy3 and Cy5, respectively). In all cases, laser illumination was done sequentially for the imaging of each optical slice. Confocal aperture was set optimally for each lens and the empirically-calculated point spread function was used to set the step size, as previously reported (Prakash et al., 1993; 1994; Sieck et al., 1999). Laser intensity and photomultiplier settings were adjusted to maintain black level on the blank sections (no primary antibody) to less than 10% of the dynamic range and to prevent saturation. All PhrMn were visualized in the rostrocaudal direction using Fluoview software version 5.0 (Olympus). Only PhrMn with visible nuclei that were not cut during spinal cord sectioning were sampled for synaptic distribution or co-localization analyses. Registration was verified empirically using multi-wavelength micro-bead calibration techniques similar to previous reports (Prakash et al., 2000; Prakash et al., 1993; 1994; Sieck et al., 1999; Zhan et al., 2000).

Synaptic Distribution Analyses

Confocal image stacks were analyzed using Metamorph Imaging Software version 7.6 (Universal Imaging Corporation, Downingtown, PA, USA). After identifying an individual PhrMn, only NRG1-immunoreactive puncta present within 2.5 μm of the PhrMn were counted. After thresholding, all NRG1 puncta located in proximity to the PhrMn soma were counted separately from those located on PhrMn dendrites. If the puncta appeared to belong to more than one motoneuron dendrite, they were counted for both. The volume of NRG1 puncta was calculated in 3D using a comprehensive image analysis software, Analyze 9.0 (Biomedical Imaging Resource, Mayo Foundation). Semi-major and semi-minor axis diameters (in longitudinal sections) were recorded for the soma of each neuron and used to calculate somal surface area and volume assuming a prolate spheroid (Prakash et al., 1993; 1994). Primary dendrite width (measured ~15 μm from the soma) and dendrite length were recorded and used to calculate primary dendritic surface area assuming a cylinder (Prakash et al., 2000; Zhan et al., 2000). In order to compare across neurons of different sizes, the density of NRG1-immunoreactive puncta was obtained by normalizing counts to the surface area of each motoneuron compartment. A total of 9 animals were used for analysis of NRG1 distribution. Most studies (n=6 animals) were conducted in 50 μm spinal cord sections to optimize imaging of PhrMn somata and primary dendrites. Additional studies (n=3 animals) were conducted in thick (100 μm) longitudinal sections to obtain more detailed analyses of

NIH-PA Author Manuscript

NIH-PA Author Manuscript

NIH-PA Author Manuscript

dendritic arborization. Localization of NRG1 was classified into one of three motoneuron compartments: soma, primary dendrites, or secondary/higher order dendrites.

Co-localization Analyses

Confocal image stacks were manually thresholded (in 12-bit) using MetaMorph software. A count function was performed in 3D by creating a dilation shell of 2.5 μm around individual PhrMn and including all NRG1 present within the shell. The intersection between each NRG1 puncta and a synaptic bouton identified by synaptophysin, VAChT, VGLUT1 or VGLUT2 was measured. Individual synapses were considered as displaying co-localization if NRG1 and the synaptic marker were present within the same anatomical structure and had at least 50% intersection. Animals were used in as many analyses as possible provided that a sufficient sample of spinal cord sections containing retrogradely labeled PhrMn could be evaluated per animal (~15 motoneurons). A total of 11 animals were used in co-localization studies (6 of these were also used in the NRG1 distribution analyses above): 4 for synaptophysin, 5 for VAChT, 3 for VGLUT1, and 4 for VGLUT2.

Statistical Analysis

All statistical analyses were conducted using JMP 8.0 (SAS Institute Inc, Cary, NC). Data are reported as mean ± standard deviation (SD), unless otherwise specified. All data represent the grand sample means per animal for all of their motoneurons. For instance, proportions of synapses displaying co-localization were calculated per motoneuron and all motoneuron proportions were averaged per animal. One-way ANOVA was used to determine differences between NRG1 distribution around the soma, primary and more distal dendrites. Pearson's correlation coefficient was used in comparisons of motoneuron size and NRG1 synaptic density at the different motoneuron compartments. In all cases, a $p \leq 0.05$ was considered significant.

Photomicrograph Production

Using Fluoview software, all confocal images were stored as 12-bit multi-TIFF files. For the purposes of image production, each multicolor confocal stack was separated into individual colors (channels) in Metamorph and, if indicated in the Figure legend, a maximum projection was produced for each individual channel in Metamorph. Individual images were exported into Adobe Photoshop (version 7.0) as TIFF and then down-converted into 8-bit for presentation only. Each channel was pseudocolored in Adobe Photoshop by changing the color gamut (RGB). Only brightness and contrast levels were adjusted linearly if needed to facilitate presentation of multiple colors.

RESULTS

Labeling of PhrMn by Intramuscular Injection

As expected based on previous extensive experience with the retrograde labeling technique (Kinkead et al., 1998; Mantilla et al., 2009; Prakash et al., 2000), PhrMn labeling by cholera toxin B was robust, allowing individual PhrMn to be easily identified. PhrMn were clustered in a rostrocaudal column in the gray matter of the cervical spinal cord, and the soma and primary dendrites were clearly visible. In order to obtain detailed information on higher order dendrites, 100 μm longitudinal sections were used. Using these sections, second and third order branches were discernible with occasional visualization of more distal dendrites. The size and distribution of PhrMn were consistent with previous reports (Lindsay et al., 1991; Prakash et al., 2000; Prakash et al., 1993; 1994). In 301 retrogradely labeled PhrMn (n=6 animals), average soma surface area was 1,996 ± 530 μm^2 and average soma volume was 8,311 ± 3,427 μm^3. The average diameter for primary dendrites was 4.3 ± 0.7 μm.

NIH-PA Author Manuscript

NIH-PA Author Manuscript

NIH-PA Author Manuscript

NRG1 Presence at Spinal Cord Motoneuron Synapses

NRG1 immunoreactivity had a punctate appearance, and was visible only in the ventral horn of the cervical spinal cord (Fig. 2 A). NRG1 puncta were found surrounding the soma and primary dendrites of large neurons in Rexed's laminae VIII and IX (Fig. 2 B). NRG1-immunoreactive puncta were found surrounding the rostrocaudal column of retrogradely labeled PhrMn, but were not restricted to PhrMn (Fig. 3). NRG1 puncta were generally oblong, with an average volume (390 puncta, n=3 animals) of 9.7 ± 5.3 μm^3 and an average maximal diameter of 2.6 ± 0.8 μm. These dimensions are consistent with the size of synaptic terminals previously identified using electron microscopy techniques (Ellenberger et al., 1990;Tai and Goshgarian, 1996).

In order to evaluate whether NRG1 puncta were synaptic sites, we examined the co-localization of NRG1 with synaptophysin in the vicinity of identified motoneurons (Fig. 4). Consistent with previous reports (Hellstrom et al., 1999;Herzog et al., 2004), synaptophysin-immunoreactive synaptic boutons were widely distributed throughout the gray matter of the spinal cord. All NRG1-containing puncta surrounding PhrMn (within 2.5 μm of soma or dendrites) co-localized with synaptophysin-immunoreactive boutons (99 motoneurons, n=4 animals). Although NRG1 and synaptophysin immunoreactivity showed only partial spatial (3-D) overlap, they were clearly present in the same anatomical structure in all cases. Consistent with the more disperse appearance of NRG1-immunoreactive synapses at PhrMn, most synaptophysin-labeled boutons did not co-localize with NRG1. Overall, 28 ± 3% of synapses on the soma or primary dendrites of PhrMn co-expressed NRG1.

NRG1 Synapses at PhrMn Soma and Primary Dendrites

The distribution of NRG1 synapses was examined using 50 μm longitudinal sections containing retrogradely-labeled PhrMn (301 motoneurons, n=6 animals). Overall, 25 ± 9 NRG1-containing synapses were present at PhrMn somata, with an average density of 0.012 ± 0.001 synapses/μm^2. The number of NRG1-immunoreactive synapses correlated with soma surface area (Fig. 5 A), such that larger PhrMn have more NRG1-containing synapses on their somata than smaller motoneurons ($p \leq 0.05$).

NRG1 was also found around PhrMn dendrites. NRG1 synapse counts were limited to motoneurons with dendrites that could be uniquely identified within a motoneuron cluster. On average, there were 7 ± 1 NRG1-containing synapses at PhrMn primary dendrites, with a density of 0.022 ± 0.001 synapses/μm^2 (304 primary dendrites at 121 motoneurons; n =6 animals). Similar to the results at the soma, the number of NRG1-immunoreactive synapses also correlated with dendritic surface area (Fig. 5 B). The density of NRG1 synapses at primary dendrites was significantly higher than at the soma of PhrMn ($p<0.001$).

In 50 μm sections, the close apposition of PhrMn within a cluster would frequently preclude detailed analyses of NRG1 distribution along the dendritic tree. We were able to obtain more detailed analysis of NRG1 synapses surrounding secondary and other higher order dendritic branches by analyzing confocal images of individual PhrMn obtained from 100 μm longitudinal sections (Fig. 6). There were relatively few NRG1 synapses at secondary and higher order dendrites (Fig. 6 A). Thus, three compartments were analyzed for NRG1 distribution within 2.5 μm of 26 reconstructed motoneurons (n=3 animals): soma, primary dendrites, and distal dendrites. Approximately half of NRG1-immunoreactive synapses were found around the primary dendrites of a PhrMn, and over 90% were found at the soma and primary dendrites (Fig. 6 B). These results are consistent with the distribution of NRG1 synapses around proximal areas of motoneurons in Rexed's laminae VIII and IX (Fig. 2). There was a statistically significant difference in the proportion of NRG1-immunoreactive synapses along the different regions of the motoneuron ($p<0.001$), with a significantly lower

NIH-PA Author Manuscript

NIH-PA Author Manuscript

NIH-PA Author Manuscript

proportion of NRG1 synapses at distal dendrites compared to the soma or primary dendrites of PhrMn ($p<0.05$).

NRG1 Co-localization with Cholinergic Synapses

The appearance of NRG1 synapses was similar to previous descriptions of cholinergic synapses on motoneurons (Hellstrom et al., 2003; Herzog et al., 2004). The vesicular acetylcholine transporter VAChT was used to determine co-localization of NRG1 with cholinergic synapses (Fig. 7). VAChT is mainly located on the membrane of cholinergic synaptic vesicles where it functions to accumulate acetylcholine (Erickson et al., 1994). Consistent with previous reports of VAChT distribution in the spinal cord ventral horn (Hellstrom et al., 2003; Herzog et al., 2004), VAChT-containing synapses were disperse around motoneurons and found predominantly around motoneuron somata and primary dendrites (Fig. 7 A). NRG1- and VAChT-immunoreactive boutons clearly belonged to the same anatomical structure (Fig. 7 B), with NRG1 partially intersecting and encasing VAChT. Overall, 75 ± 14 % of NRG1 synapses within 2.5 μm of a PhrMn, were present at VAChT-immunoreactive synaptic sites (71 motoneurons, n=5 animals). In addition, nearly all (99 ± 1%) VAChT synaptic boutons at PhrMn co-expressed NRG1.

NRG1 Co-localization with Glutamatergic Synapses

In the present study, we used the vesicular glutamate transporters VGLUT1 and VGLUT2 to identify glutamatergic synapses at motoneurons. The appearance and distribution of glutamatergic boutons around PhrMn was similar to that reported in previous studies in the spinal cord ventral horn (Herzog et al., 2004; Oliveira et al., 2003), and in agreement with these previous reports, VGLUT2 appeared more abundant than VGLUT1. In addition, both VGLUT1- and VGLUT2-immunoreactive boutons appeared to be smaller yet more abundant than VAChT- or NRG1-containing synapses. In 64 motoneurons (n=3 animals), we found no evidence of NRG1 co-localization with VGLUT1 (Fig. 8 A). VGLUT2-immunoreactive boutons showed partial intersection with NRG1 such that 26 ± 6% of NRG1-containing synapses were present at glutamatergic sites labeled by VGLUT-2 (69 motoneurons, n=4 animals; Fig. 8 B). Overall, only ~6 % of glutamatergic synapses within 2.5 μm of PhrMn soma and dendrites co-localized with NRG1.

DISCUSSION

The distribution of NRG1 synapses around motoneurons and the association of NRG1 with specific neurotransmitter systems provide important information necessary to elucidate the possible role of NRG1 in the adult neuromuscular system. To the best of our knowledge, this is the first study to show that NRG1 is found in synapses present around motoneurons in the ventral horn of the spinal cord and specifically at PhrMn. The majority of NRG1 was distributed at the soma and primary dendrites of PhrMn with very few NRG1-immunoreactive synapses in the more distal dendritic areas. We also found that NRG1 is associated predominantly with cholinergic synaptic terminals, and a subset of glutamatergic terminals. In previous studies, NRG1 was found to play an important role in the development and regulation of cholinergic neurotransmission at the neuromuscular junction (Jo et al., 1995; Loeb et al., 2002; Sandrock et al., 1997; Zhu et al., 1995) and in the hippocampus (Chang and Fischbach, 2006; Zhong et al., 2008). In addition, NRG1 was reported to be important for glutamatergic neurotransmission in the cerebellum (Ozaki et al., 1997; Ozaki et al., 2000) and hippocampus (Li et al., 2007). Although these studies highlighted the importance of NRG1 in the development of cholinergic and glutamatergic synapses, NRG1 expression in the adult neuromuscular system had not been previously characterized.

NIH-PA Author Manuscript

NIH-PA Author Manuscript

NIH-PA Author Manuscript

Using immunohistochemical methods and 3D confocal microscopy, we found that NRG1 is present at synapses on large neurons in the spinal cord ventral horn. Although only 60–70% of the PhrMn present in the rat are labeled by intramuscular cholera toxin injection (Mantilla et al., 2009), we expect that both unlabeled PhrMn and other motoneurons also have NRG1 surrounding them. In fact, NRG1 was present exclusively in Rexed's laminae VIII and IX (Fig. 2 A), predominantly around the soma and primary dendrites of motoneurons.

Synaptic Localization of NRG1

NRG1 has widespread distribution in the adult brain with mRNA expression in many different areas including the hippocampus, dorsolateral prefrontal cortex and cerebellum (Law et al., 2004). Previous studies examining synaptic effects of NRG1 have not consistently determined NRG1 localization at specific CNS synapses. In the cerebellum, NRG1 was shown to be concentrated at synapses between mossy fibers and cerebellar granule cells (Ozaki et al., 2000). Although NRG1 plays an important role in regulating glutamatergic and cholinergic transmission in the hippocampus (Chang and Fischbach, 2006; Li et al., 2007), it is not clear where NRG1 is located at these synapses. Immunohistochemical staining in the hippocampus and prefrontal cortex suggests primarily labeling of neurons (e.g., interneurons, pyramidal and granule cells) and axonal fibers (Bernstein et al., 2006), but not specifically synaptic sites. Since synapses have been shown using scanning electron microscopy to be 0.5–2.2 μm in length and 0.5–1.5 μm in width (Ellenberger et al., 1990; Tai and Goshgarian, 1996), we specifically examined NRG1 distribution within 2.5 μm of identified, retrogradely labeled PhrMn. We found that, in agreement with our hypothesis, NRG1 expression is present at synapses labeled with synaptophysin. Indeed, all NRG1 was found to co-localize with synaptophysin-labeled boutons (Fig. 4). Furthermore, NRG1 synapses comprised ~28% of the total synaptic sites on PhrMn soma or primary dendrites.

Diffraction limits of optical fluorescence microscopy preclude unequivocal ascertainment of the pre- vs. post-synaptic localization of NRG1 on motoneurons (XY resolution ~ 0.3 μm). At the neuromuscular junction it is thought that motoneuron-derived NRG1 acts on skeletal muscle fibers to increase expression and clustering of cholinergic receptors (Jo et al., 1995; Loeb et al., 2002; Sandrock et al., 1997; Zhu et al., 1995). However, the pre- vs. post-synaptic localization of NRG1 at the neuromuscular junction is not clear (Goodearl et al., 1995; Jaworski and Burden, 2006). It is not clear if NRG1 is presynaptic at hippocampus or cerebellar synapses, but a postsynaptic effect is usually reported (Chang and Fischbach, 2006; Ozaki et al., 2000). In addition, based on the co-localization of NRG1 with presynaptic elements such as the neurotransmitter transporters VAChT and VGLUT2, it is possible that NRG1 is presynaptic at PhrMn. Nonetheless, future studies using higher resolution techniques such as immuno-electron microscopy are needed to specifically determine the localization of NRG1 within synapses on adult motoneurons, including PhrMn.

Distribution of NRG1 Synapses

Based on the disperse appearance of NRG1 within Rexed's laminae VIII and IX (Fig. 2), NRG1-expressing synaptic sites seem to surround the soma and proximal dendrites of motoneurons. In PhrMn, we directly examined the distribution of NRG1 synapses along the different motoneuron compartments using thick longitudinal spinal cord sections (Fig. 6). To date, detailed analyses of the distribution of NRG1 or other trophic factors on motoneurons have not been reported. Although synaptic NRG1 was reported in the cerebellum (Ozaki et al., 2000), these investigators did not determine the relationship between synapses expressing NRG1 and their localization along the dendritic tree. In the present study, we found that NRG1 is located predominantly at synapses on the soma and primary dendrites of

NIH-PA Author Manuscript

NIH-PA Author Manuscript

NIH-PA Author Manuscript

PhrMn (>90% of NRG1 synapses), with a significantly higher density of NRG1 synapses at primary dendrites than at the soma. The proximal distribution of NRG1 synapses suggests an important role in regulating motoneuron excitability, since motoneuron modeling studies report that synaptic inputs at primary dendrites and soma exert a disproportionately larger influence on motoneuron output (Cushing et al., 2005;Vieira and Kohn, 2007). Consistent with a general role of NRG1 in regulating motoneuron excitability, the number of NRG1-immunoreactive sites at the soma and primary dendrites of PhrMn changed proportionately with motoneuron size (i.e., surface area; Fig. 5). Future studies must address whether NRG1 modulates the expression or function of specific neurotransmitter receptors that would regulate motoneuron excitability, especially since NRG1 is known to regulate both cholinergic and glutamatergic transmission in other CNS regions (Chang and Fischbach, 2006;Li et al., 2007;Ozaki et al., 1997).

To date, there is insufficient information regarding the specific distribution of neurotransmitter or trophic factor inputs onto motoneurons (Mantilla and Sieck, 2008). In particular, methods providing detailed anatomical information on dendritic arborization of motoneurons (in 3D) have not been combined with immunohistochemical localization of specific neurotransmitters or trophic factor inputs. In one series of studies, Shigenaga and colleagues completed detailed EM analyses of excitatory and inhibitory synaptic bouton distribution along the dendritic tree of a very small sample of motoneurons involved in the control of jaw movements (n=4 masseter motoneurons and n=2 jaw opening motoneurons). Only a subset of primary, intermediate or distal dendrites were examined for synaptic localization since their methods did not allow comprehensive analyses nor 3D reconstructions of dendritic trees. Glutamatergic inputs were found to be more abundant around distal and intermediate dendrites rather than the primary dendrites or soma (Bae et al., 1999; Shigenaga et al., 2005). In other investigations, cholinergic inputs on motoneurons were described as being restricted to proximal neuronal compartments, but detailed analyses of synaptic distribution were not conducted (Hellstrom et al., 1999; Miles et al., 2007; Zagoraiou et al., 2009).

A method such as that developed in the present study for analysis of NRG1 distribution on motoneurons may be potentially useful in obtaining quantitative information regarding the distribution of other synaptic inputs (e.g., specific neurotransmitter systems). However, limitations of the retrograde labeling technique may impair the ability to properly visualize distal dendrites and hence analyze synaptic distribution around them. The use of more robust labeling techniques (i.e., based on intracellular injection) could overcome such limitations.

NRG1 Co-Expression with Neurotransmitter Inputs on Motoneurons

Multiple studies have reported widespread distribution of both glutamatergic and cholinergic synaptic inputs on motoneurons (Bae et al., 1999; Herzog et al., 2004; Landry et al., 2004; Shigenaga et al., 2005), including PhrMn (McCrimmon et al., 1989; Murphy et al., 1996; Tai and Goshgarian, 1996; Zhan et al., 1989). Synaptic inputs to PhrMn also consist of serotonin, GABA, glycine, substance P, and various opioid peptides (Zhan et al., 1989). In the present study, we found a strong association between cholinergic synaptic inputs and NRG1 expression at PhrMn. Approximately 75% of NRG1 synapses co-expressed VAChT, and essentially all cholinergic synapses at PhrMn co-expressed NRG1. We also found that ~25% of NRG1 synapses co-expressed VGLUT2 (none co-expressed VGLUT1), but overall only ~6% of glutamatergic synapses at the PhrMn soma or primary dendrites co-expressed NRG1. Thus, all NRG1-immunoreactive synapses on PhrMn could be accounted for by VAChT and VGLUT2 synaptic sites. Although we did not conduct the multi-labeling experiments necessary to exclude any synaptic co-localization of VAChT and VGLUT2, these different neurotransmitter inputs have distinct morphology (Fig. 7; and Fig. 8). Furthermore, previous studies suggest there is no co-localization between VAChT,

NIH-PA Author Manuscript

NIH-PA Author Manuscript

NIH-PA Author Manuscript

VGLUT1 or VGLUT2 around putative spinal motoneurons (Herzog et al., 2004; Oliveira et al., 2003). The association of NRG1 expression with specific neurotransmitter synapses suggests an important role for NRG1 in the development or maintenance and regulation of these synapses in the adult, subjects that future studies should address directly.

Several studies show that acetylcholine plays an important role in the integration of excitatory drive to motoneurons (Miles et al., 2007; Zagoraiou et al., 2009). Cholinergic projections to PhrMn from raphe nuclei appear to be predominantly nicotinic (Dehkordi et al., 2004), and NRG1 is known to modulate nicotinic acetylcholine receptor (nAChR) expression at neuromuscular junctions (Jo et al., 1995; Loeb et al., 2002; Sandrock et al., 1997) and α_7-nAChR-mediated currents in the hippocampus (Chang and Fischbach, 2006; Zhong et al., 2008). Other cholinergic inputs to motoneurons, classically described as large “C boutons”, contact the soma and proximal dendrites (Borges and Iversen, 1986; Hellstrom et al., 1999; Herzog et al., 2004; Ichikawa et al., 1997) and resemble NRG1 puncta described in the present study. These C boutons are known to be associated with postsynaptic muscarinic M2 receptors (Hellstrom et al., 2003; Muennich and Fyffe, 2004) and the voltage-gated potassium channel subunit $K_v2.1$, with delayed rectifier properties (Wilson et al., 2004), and may thus modulate motoneuron excitability. C boutons are thought to originate from an intraspinal source (Hellstrom et al., 2003), with a recent study suggesting that a small cluster of spinal cholinergic interneurons, $V0_C$ neurons, are the sole source of C bouton inputs to motoneurons (Zagoraiou et al., 2009). C bouton inputs to motoneurons reportedly increase motoneuron excitability during rhythmic motor behaviors (Miles et al., 2007; Zagoraiou et al., 2009). The similar morphology and close association of NRG1 with cholinergic synaptic inputs on PhrMn suggests that NRG1 could play an important role in the development of C bouton synapses. Specific information regarding the co-localization of NRG1 with α_7-nAChR and/or M2 AChR will be important to understand the role of NRG1 at motoneurons.

In the present study, the transporters VGLUT1 and VGLUT2 were used to identify glutamatergic inputs on PhrMn. We found that NRG1 is associated with a small, yet centrally-located subset of glutamatergic terminals expressing VGLUT2 (~6% of glutamatergic inputs on soma or primary dendrites of PhrMn; Fig. 8 B). Most glutamatergic inputs on jaw motoneurons were found to be around distal and intermediate dendrites rather than the primary dendrites or soma (Bae et al., 1999;Shigenaga et al., 2005), but these investigators did not differentiate VGLUT1 vs. VGLUT2 terminals. Even though both VGLUT1 and VGLUT2 share 79% amino acid identity in rat (Bai et al., 2001), their expression patterns differ in various areas of the nervous system (Alvarez et al., 2004;Herzog et al., 2004;Herzog et al., 2006;Oliveira et al., 2003). In particular, VGLUT2 is more abundant in laminae VIII and IX of the spinal cord (Alvarez et al., 2004;Oliveira et al., 2003), suggesting a specific role of VGLUT2 at motoneurons. However, not much is known about the potentially different roles of these two transporters in glutamatergic transmission. Regardless, NRG1 was shown to control the expression of different glutamatergic NMDA receptor subunits during the development of mossy fiber-granule cell synapses in the cerebellum (Ozaki et al., 1997;Ozaki et al., 2000). In the hippocampus, NRG1 signaling via postsynaptic ErbB4 receptors was reported to be critical for enhanced glutamatergic transmission (Li et al., 2007). Of note, glutamatergic NMDA receptors are necessary for the long-term facilitation of phrenic motor output induced by intermittent hypoxia (McGuire et al., 2008;McGuire et al., 2005), suggesting that NRG1 may play an important role in the integration of excitatory drive to motoneurons.

In summary, we found that NRG1 is present at cholinergic and glutamatergic synapses on PhrMn in the ventral horn of the spinal cord. Furthermore, NRG1 is distributed predominantly at the soma and primary dendrites rather than higher order dendrites. The

NIH-PA Author Manuscript

NIH-PA Author Manuscript

NIH-PA Author Manuscript

characterization of NRG1 distribution and its association with specific neurotransmitter pathways is a crucial step in determining the role of NRG1 signaling in adult neuromuscular systems.

Acknowledgments

The authors would like to thank Drs. Heather M. Argadine and Leonid G. Ermilov for their scientific input and relevant discussion, and Ms. Yun-Hua Fang for technical assistance.

Supported by NIH grants AR051173-S1, HL096750, the Paralyzed Veterans of America Research Foundation and Mayo Clinic.

References

Alvarez FJ, Villalba RM, Zerda R, Schneider SP. Vesicular glutamate transporters in the spinal cord, with special reference to sensory primary afferent synapses. Journal of Comparative Neurology. 2004; 472(3):257–280. [PubMed: 15065123]

Bae YC, Nakamura T, Ihn HJ, Choi MH, Yoshida A, Moritani M, Honma S, Shigenaga Y. Distribution pattern of inhibitory and excitatory synapses in the dendritic tree of single masseter alpha-motoneurons in the cat. Journal of Comparative Neurology. 1999; 414(4):454–468. [PubMed: 10531539]

Bai L, Xu H, Collins JF, Ghishan FK. Molecular and functional analysis of a novel neuronal vesicular glutamate transporter. J Biol Chem. 2001; 276(39):36764–36769. [PubMed: 11432869]

Bernstein HG, Lendeckel U, Bertram I, Bukowska A, Kanakis D, Dobrowolny H, Stauch R, Krell D, Mawrin C, Budinger E, Keilhoff G, Bogerts B. Localization of neuregulin-1alpha (heregulin-alpha) and one of its receptors, ErbB-4 tyrosine kinase, in developing and adult human brain. Brain Research Bulletin. 2006; 69(5):546–559. [PubMed: 16647583]

Borges LF, Iversen SD. Topography of choline acetyltransferase immunoreactive neurons and fibers in the rat spinal cord. Brain Research. 1986; 362(1):140–148. [PubMed: 3510688]

Buonanno A, Fischbach GD. Neuregulin and ErbB receptor signaling pathways in the nervous system. Current Opinion in Neurobiology. 2001; 11(3):287–296. [PubMed: 11399426]

Chang Q, Fischbach GD. An acute effect of neuregulin 1 beta to suppress alpha 7-containing nicotinic acetylcholine receptors in hippocampal interneurons. Journal of Neuroscience. 2006; 26(44):11295–11303. [PubMed: 17079657]

Cushing S, Bui T, Rose PK. Effect of nonlinear summation of synaptic currents on the input-output properties of spinal motoneurons. Journal Of Neurophysiology. 2005; 94(5):3465–3478. [PubMed: 16079193]

Dehkordi O, Haxhiu MA, Millis RM, Dennis GC, Kc P, Jafri A, Khajavi M, Trouth CO, Zaidi SI. Expression of alpha-7 nAChRs on spinal cord-brainstem neurons controlling inspiratory drive to the diaphragm. Respir Physiol Neurobiol. 2004; 141(1):21–34. [PubMed: 15234673]

Ellenberger HH, Feldman JL, Goshgarian HG. Ventral respiratory group projections to phrenic motoneurons: electron microscopic evidence for monosynaptic connections. Journal of Comparative Neurology. 1990; 302(4):707–714. [PubMed: 1707065]

Erickson JD, Varoqui H, Schafer MK, Modi W, Diebler MF, Weihe E, Rand J, Eiden LE, Bonner TI, Usdin TB. Functional identification of a vesicular acetylcholine transporter and its expression from a “cholinergic” gene locus. J Biol Chem. 1994; 269(35):21929–21932. [PubMed: 8071310]

Falls DL. Neuregulins: functions, forms, and signaling strategies. Exp Cell Res. 2003; 284(1):14–30. [PubMed: 12648463]

Goodearl AD, Yee AG, Sandrock AW Jr. Corfas G, Fischbach GD. ARIA is concentrated in the synaptic basal lamina of the developing chick neuromuscular junction. J Cell Biol. 1995; 130(6):1423–1434. [PubMed: 7559763]

Hellstrom J, Arvidsson U, Elde R, Cullheim S, Meister B. Differential expression of nerve terminal protein isoforms in VAChT-containing varicosities of the spinal cord ventral horn. Journal of Comparative Neurology. 1999; 411(4):578–590. [PubMed: 10421869]

NIH-PA Author Manuscript

NIH-PA Author Manuscript

NIH-PA Author Manuscript

Hellstrom J, Oliveira AL, Meister B, Cullheim S. Large cholinergic nerve terminals on subsets of motoneurons and their relation to muscarinic receptor type 2. Journal of Comparative Neurology. 2003; 460(4):476–486. [PubMed: 12717708]

Herzog E, Landry M, Buhler E, Bouali-Benazzouz R, Legay C, Henderson CE, Nagy F, Dreyfus P, Giros B, El Mestikawy S. Expression of vesicular glutamate transporters, VGLUT1 and VGLUT2, in cholinergic spinal motoneurons. European Journal of Neuroscience. 2004; 20(7):1752–1760. [PubMed: 15379996]

Herzog E, Takamori S, Jahn R, Brose N, Wojcik SM. Synaptic and vesicular co-localization of the glutamate transporters VGLUT1 and VGLUT2 in the mouse hippocampus. J Neurochem. 2006; 99(3):1011–1018. [PubMed: 16942593]

Ichikawa T, Ajiki K, Matsuura J, Misawa H. Localization of two cholinergic markers, choline acetyltransferase and vesicular acetylcholine transporter in the central nervous system of the rat: in situ hybridization histochemistry and immunohistochemistry. J Chem Neuroanat. 1997; 13(1):23–39. [PubMed: 9271193]

Jaworski A, Burden SJ. Neuromuscular synapse formation in mice lacking motor neuron- and skeletal muscle-derived Neuregulin-1. Journal of Neuroscience. 2006; 26(2):655–661. [PubMed: 16407563]

Jo SA, Zhu X, Marchionni MA, Burden SJ. Neuregulins are concentrated at nerve-muscle synapses and activate ACh-receptor gene expression. Nature. 1995; 373(6510):158–161. [PubMed: 7816098]

Kerber G, Streif R, Schwaiger FW, Kreutzberg GW, Hager G. Neuregulin-1 isoforms are differentially expressed in the intact and regenerating adult rat nervous system. J Mol Neurosci. 2003; 21(2): 149–165. [PubMed: 14593214]

Kinkead R, Zhan WZ, Prakash YS, Bach KB, Sieck GC, Mitchell GS. Cervical dorsal rhizotomy enhances serotonergic innervation of phrenic motoneurons and serotonin-dependent long-term facilitation of respiratory motor output in rats. Journal of Neuroscience. 1998; 18(20):8436–8443. [PubMed: 9763486]

Knaus P, Betz H. Mapping of a dominant immunogenic region of synaptophysin, a major membrane protein of synaptic vesicles. FEBS Letter. 1990; 261(2):358–360.

Landry M, Bouali-Benazzouz R, El Mestikawy S, Ravassard P, Nagy F. Expression of vesicular glutamate transporters in rat lumbar spinal cord, with a note on dorsal root ganglia. Journal of Comparative Neurology. 2004; 468(3):380–394. [PubMed: 14681932]

Law AJ, Shannon Weickert C, Hyde TM, Kleinman JE, Harrison PJ. Neuregulin-1 (NRG-1) mRNA and protein in the adult human brain. Neuroscience. 2004; 127(1):125–136. [PubMed: 15219675]

Li B, Woo RS, Mei L, Malinow R. The neuregulin-1 receptor erbB4 controls glutamatergic synapse maturation and plasticity. Neuron. 2007; 54(4):583–597. [PubMed: 17521571]

Lindholm T, Cullheim S, Deckner M, Carlstedt T, Risling M. Expression of neuregulin and ErbB3 and ErbB4 after a traumatic lesion in the ventral funiculus of the spinal cord and in the intact primary olfactory system. Exp Brain Res. 2002; 142(1):81–90. [PubMed: 11797086]

Lindsay AD, Greer JJ, Feldman JL. Phrenic motoneuron morphology in the neonatal rat. Journal of Comparative Neurology. 1991; 308:169–179. [PubMed: 1716267]

Loeb JA, Hmadcha A, Fischbach GD, Land SJ, Zakarian VL. Neuregulin expression at neuromuscular synapses is modulated by synaptic activity and neurotrophic factors. Journal of Neuroscience. 2002; 22(6):2206–2214. [PubMed: 11896160]

Mantilla CB, Sieck GC. Trophic factor expression in phrenic motor neurons. Respir Physiol Neurobiol. 2008; 164(1–2):252–262. [PubMed: 18708170]

Mantilla CB, Zhan WZ, Sieck GC. Retrograde labeling of phrenic motoneurons by intrapleural injection. Journal of Neuroscience Methods. 2009; 182:244–249. [PubMed: 19559048]

McCrimmon DR, Smith JC, Feldman JL. Involvement of excitatory amino acids in neurotransmission of inspiratory drive to spinal respiratory motoneurons. Journal of Neuroscience. 1989; 9(6):1910–1921. [PubMed: 2542482]

McGuire M, Liu C, Cao Y, Ling L. Formation and maintenance of ventilatory long-term facilitation require NMDA but not non-NMDA receptors in awake rats. Journal of Applied Physiology. 2008; 105(3):942–950. [PubMed: 18583381]

NIH-PA Author Manuscript

NIH-PA Author Manuscript

NIH-PA Author Manuscript

McGuire M, Zhang Y, White DP, Ling L. Phrenic long-term facilitation requires NMDA receptors in the phrenic motonucleus in rats. J Physiol. 2005; 567(Pt 2):599–611. [PubMed: 15932891]

Mekalanos JJ, Collier RJ, Romig WR. Purification of cholera toxin and its subunits: new methods of preparation and the use of hypertoxinogenic mutants. Infect Immun. 1978; 20(2):552–558. [PubMed: 669812]

Miles GB, Hartley R, Todd AJ, Brownstone RM. Spinal cholinergic interneurons regulate the excitability of motoneurons during locomotion. Proc Natl Acad Sci U S A. 2007; 104(7):2448–2453. [PubMed: 17287343]

Muennich EA, Fyffe RE. Focal aggregation of voltage-gated, Kv2.1 subunit-containing, potassium channels at synaptic sites in rat spinal motoneurones. J Physiol. 2004; 554(Pt 3):673–685. [PubMed: 14608003]

Murphy SM, Pilowsky PM, Llewellyn-Smith IJ. Vesicle shape and amino acids in synaptic inputs to phrenic motoneurons: do all inputs contain either glutamate or GABA? Journal of Comparative Neurology. 1996; 373(2):200–219. [PubMed: 8889922]

Oliveira AL, Hydling F, Olsson E, Shi T, Edwards RH, Fujiyama F, Kaneko T, Hokfelt T, Cullheim S, Meister B. Cellular localization of three vesicular glutamate transporter mRNAs and proteins in rat spinal cord and dorsal root ganglia. Synapse. 2003; 50(2):117–129. [PubMed: 12923814]

Ozaki M, Sasner M, Yano R, Lu HS, Buonanno A. Neuregulin-beta induces expression of an NMDA-receptor subunit. Nature. 1997; 390(6661):691–694. [PubMed: 9414162]

Ozaki M, Tohyama K, Kishida H, Buonanno A, Yano R, Hashikawa T. Roles of neuregulin in synaptogenesis between mossy fibers and cerebellar granule cells. J Neurosci Res. 2000; 59(5): 612–623. [PubMed: 10686589]

Prakash YS, Mantilla CB, Zhan WZ, Smithson KG, Sieck GC. Phrenic motoneuron morphology during rapid diaphragm muscle growth. Journal of Applied Physiology. 2000; 89(2):563–572. [PubMed: 10926639]

Prakash YS, Smithson KG, Sieck GC. Measurements of motoneuron somal volumes using laser confocal microscopy: comparisons with shape-based stereological estimations. Neuroimage. 1993; 1(2):95–107. [PubMed: 9343561]

Prakash YS, Smithson KG, Sieck GC. Application of the Cavalieri principle in volume estimation using laser confocal microscopy. Neuroimage. 1994; 1(4):325–333. [PubMed: 9343582]

Rappaport RS, Rubin BA, Tint H. Development of a purified cholera toxoid. I. Purification of toxin. Infect Immun. 1974; 9(2):294–303. [PubMed: 4205945]

Ricart K, J. Pearson R J, Viera L, Cassina P, Kamaid A, Carroll SL, Estevez AG. Interactions between beta-neuregulin and neurotrophins in motor neuron apoptosis. J Neurochem. 2006; 97(1):222–233. [PubMed: 16524373]

Sandrock AW Jr. Dryer SE, Rosen KM, Gozani SN, Kramer R, Theill LE, Fischbach GD. Maintenance of acetylcholine receptor number by neuregulins at the neuromuscular junction in vivo. Science. 1997; 276(5312):599–603. [PubMed: 9110980]

Shigenaga Y, Moritani M, Oh SJ, Park KP, Paik SK, Bae JY, Kim HN, Ma SK, Park CW, Yoshida A, Ottersen OP, Bae YC. The distribution of inhibitory and excitatory synapses on single, reconstructed jaw-opening motoneurons in the cat. Neuroscience. 2005; 133(2):507–518. [PubMed: 15878646]

Sieck GC, Mantilla CB, Prakash YS. Volume measurements in confocal microscopy. Methods Enzymol. 1999; 307:296–315. [PubMed: 10506980]

Tai Q, Goshgarian HG. Ultrastructural quantitative analysis of glutamatergic and GABAergic synaptic terminals in the phrenic nucleus after spinal cord injury. Journal of Comparative Neurology. 1996; 372(3):343–355. [PubMed: 8873865]

Trinidad JC, Fischbach GD, Cohen JB. The Agrin/MuSK signaling pathway is spatially segregated from the neuregulin/ErbB receptor signaling pathway at the neuromuscular junction. Journal of Neuroscience. 2000; 20(23):8762–8770. [PubMed: 11102484]

Vieira MF, Kohn AF. Compartmental models of mammalian motoneurons of types S, FR and FF and their computer simulation. Computers in biology and medicine. 2007; 37(6):842–860. [PubMed: 17098219]

NIH-PA Author Manuscript

NIH-PA Author Manuscript

NIH-PA Author Manuscript

Wiedenmann B, Franke WW. Identification and localization of synaptophysin, an integral membrane glycoprotein of Mr 38,000 characteristic of presynaptic vesicles. Cell. 1985; 41(3):1017–1028. [PubMed: 3924408]

Wilson JM, Rempel J, Brownstone RM. Postnatal development of cholinergic synapses on mouse spinal motoneurons. Journal of Comparative Neurology. 2004; 474(1):13–23. [PubMed: 15156576]

Zagoraiou L, Akay T, Martin JF, Brownstone RM, Jessell TM, Miles GB. A cluster of cholinergic premotor interneurons modulates mouse locomotor activity. Neuron. 2009; 64(5):645–662. [PubMed: 20005822]

Zhan WZ, Ellenberger HH, Feldman JL. Monoaminergic and GABAergic terminations in phrenic nucleus of rat identified by immunohistochemical labeling. Neuroscience. 1989; 31(1):105–113. [PubMed: 2771052]

Zhan WZ, Mantilla CB, Zhan P, Bitton A, Prakash YS, de Troyer A, Sieck GC. Regional differences in serotonergic input to canine parasternal intercostal motoneurons. Journal of Applied Physiology. 2000; 88(5):1581–1589. [PubMed: 10797116]

Zhong C, Du C, Hancock M, Mertz M, Talmage DA, Role LW. Presynaptic type III neuregulin 1 is required for sustained enhancement of hippocampal transmission by nicotine and for axonal targeting of alpha7 nicotinic acetylcholine receptors. Journal of Neuroscience. 2008; 28(37):9111–9116. [PubMed: 18784291]

Zhu X, Lai C, Thomas S, Burden SJ. Neuregulin receptors, erbB3 and erbB4, are localized at neuromuscular synapses. Embo Journal. 1995; 14(23):5842–5848. [PubMed: 8846777]

NIH-PA Author Manuscript

NIH-PA Author Manuscript

NIH-PA Author Manuscript

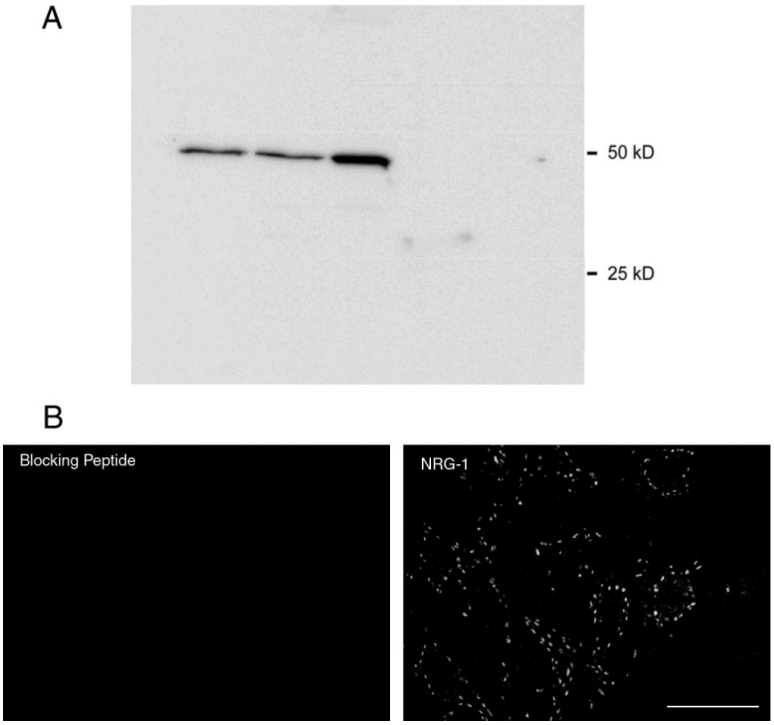

Figure 1.

Neuregulin-1 (NRG1) immunodetection

A. The NRG1 antibody (anti-neureguilin-1α/β1/2) recognizes a single protein band at ~50 kD in immunophoretically-separated rat spinal cord tissue (columns 1 and 2) and phrenic nerve (column 3), but not diaphragm muscle or undifferentiated NSC-34 cells (a neuronal hybrid cell line).

B. Single confocal slices of rat spinal cord tissue show immunohistochemical control for NRG1 immunostaining in rat spinal cord. NRG1 immunoreactivity was abolished when the diluted primary antibody was preincubated with immunizing peptide. Bar: 50 μm.

NIH-PA Author Manuscript
NIH-PA Author Manuscript
NIH-PA Author Manuscript

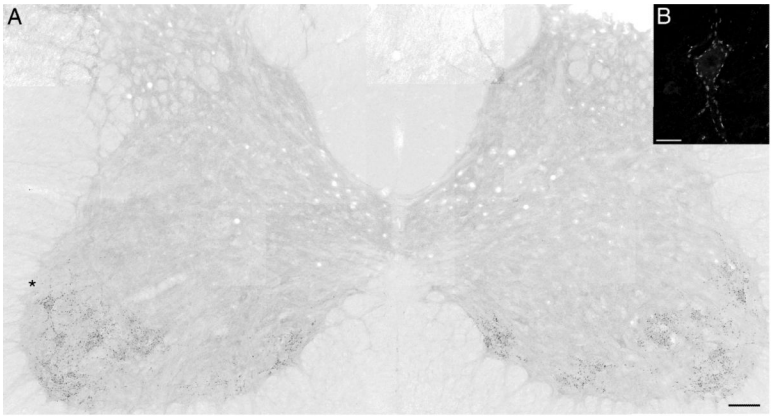

Figure 2.

Neuregulin-1 expression in the cervical spinal cord.

A. Montage of maximum intensity projections from multiple confocal image stacks obtained from a transverse section of the spinal cord (C4–C5). The NRG1 immunoreactivity (black) is punctate on the perimeter of large neurons in Rexed's laminae VIII and IX of the ventral horn of the spinal cord. The background was set to permit visualization of the gray matter in the spinal cord (orientation: dorsal is at the top of the image). This pattern of NRG1 immunoreactivity is suggestive of its presence on the surface of motoneurons. Bar: 100 μm. B. Maximum intensity projection of three confocal slices containing the neuron marked by asterisk in A. The gray level scheme was inverted to optimize visualization of NRG1 in this figure. Note that NRG1 puncta are found predominantly at the soma and primary dendrites of large neurons, likely motoneurons. Bar: 25 μm.

NIH-PA Author Manuscript

NIH-PA Author Manuscript

NIH-PA Author Manuscript

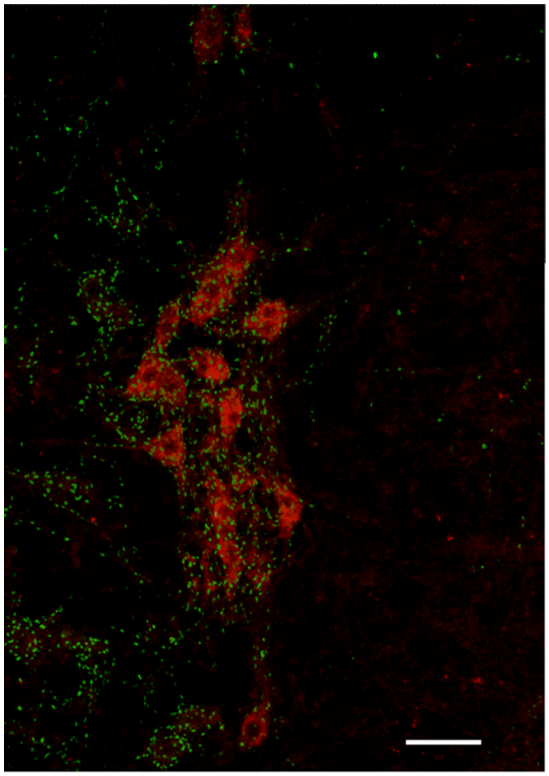

Figure 3.
NRG1 expression in the phrenic motor nucleus.
Maximum intensity projection of three confocal slices showing a longitudinal section at ~C3–4 (orientation: rostral, top; medial, left). Phrenic motoneurons (PhrMn) were retrogradely labeled by cholera toxin B (CTB; red) injected into the diaphragm muscle (see Methods). NRG1 (green) was widely distributed on PhrMn and other large neurons in the cervical ventral horn. Bar: 100 μm.

NIH-PA Author Manuscript

NIH-PA Author Manuscript

NIH-PA Author Manuscript

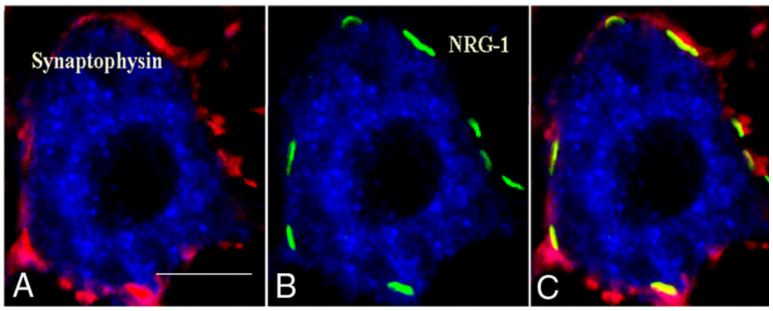

Figure 4.

NRG1-immunoreactivity at synaptic sites on PhrMn.

Maximum intensity projections of three consecutive confocal slices show presence of large number of synaptic sites labeled by synaptophysin (red; A) within 2.5 μm of the soma of a single retrogradely-labeled PhrMn (blue); relatively larger, yet more disperse, NRG1 puncta (green; B); and localization of NRG1 at synaptophysin-immunoreactive synaptic sites (C). Bar: 10 μm.

NIH-PA Author Manuscript
NIH-PA Author Manuscript
NIH-PA Author Manuscript

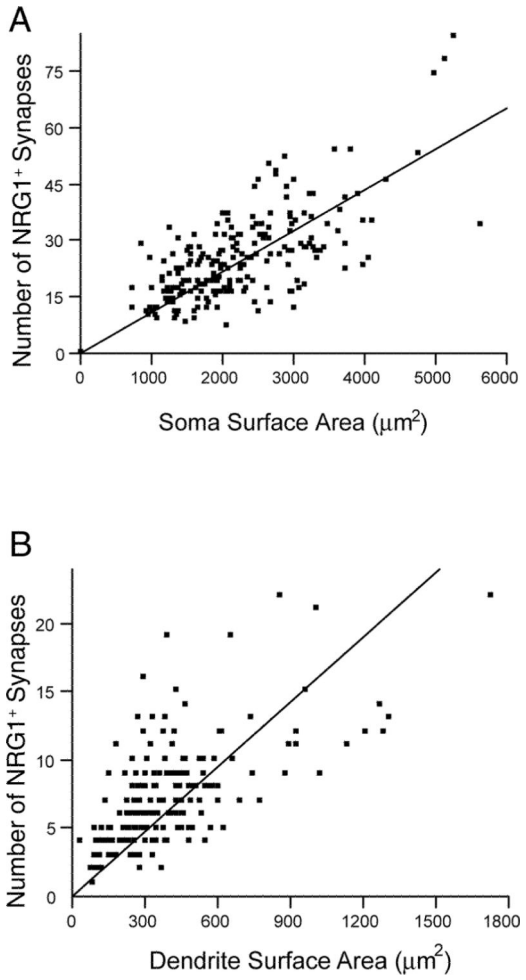

Figure 5.

Density of NRG1-containing synapses at phrenic motoneurons.

A. The number of NRG1 synapses at PhrMn soma correlates with soma surface area (r^2 = 0.45, $p<0.01$). Spearman's ρ is 0.62 ($p<0.0001$).

B. The number of NRG1 synapses at the primary dendrites of PhrMn also correlates with primary dendrite surface area (r^2 = 0.38, $p<0.01$). Spearman's ρ is 0.66 ($p<0.0001$).

NIH-PA Author Manuscript

NIH-PA Author Manuscript

NIH-PA Author Manuscript

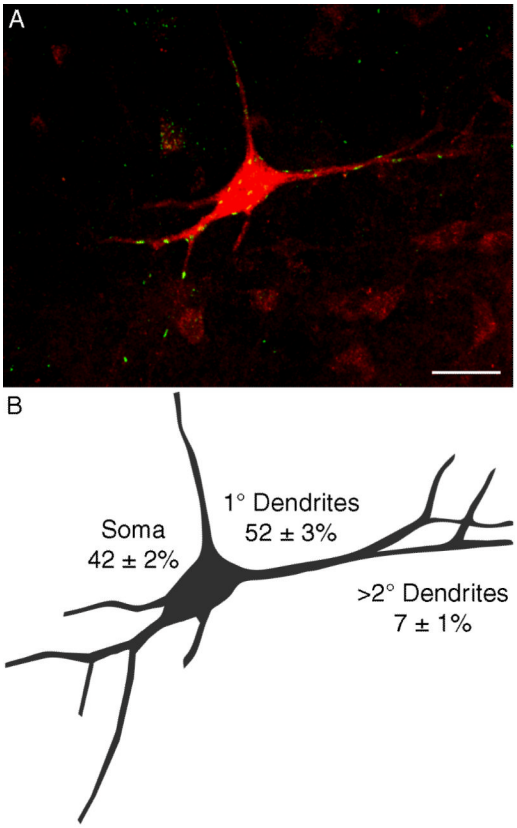

Figure 6.

Distribution of NRG1-containing synapses along motoneuron compartments.

A. Maximum intensity projection of 73 slices obtained from a 100 μm longitudinal section at C4 shows multiple NRG1-immunoreactive synapses (green) at a retrogradely labeled PhrMn (red). The background level was set to allow visualization of distal dendritic branches resulting in increased noise in the projection of this thick confocal stack. Also note that some NRG1-immunoreactive synapses may falsely appear to be within the motoneuron. The number of NRG1-expressing synaptic sites is greatest at the soma and primary dendrites. Bar: 50 μm

B. Camera lucida drawing of the motoneuron shown in A. The average (± SD) percentage of NRG1-immunoreactive synapses at the soma, primary dendrites and distal dendrites (i.e., secondary and higher order) for 26 PhrMn (n=3 animals) is indicated.

NIH-PA Author Manuscript
NIH-PA Author Manuscript
NIH-PA Author Manuscript

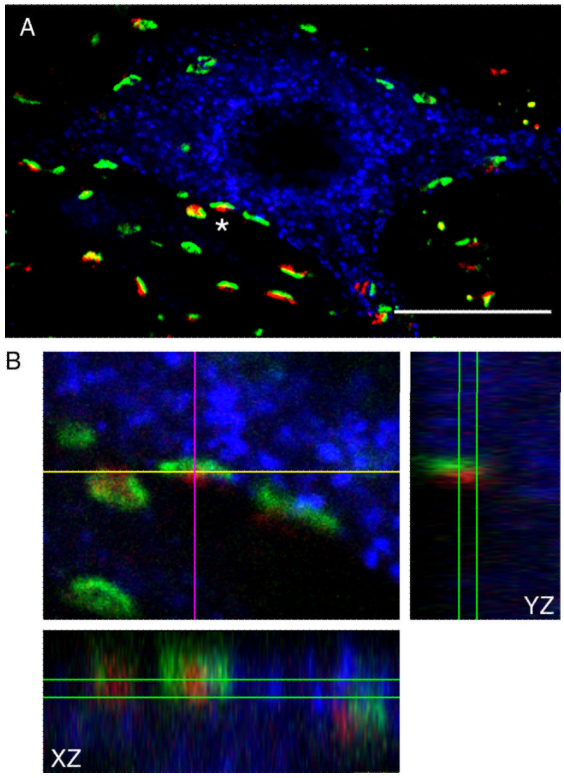

Figure 7.

Localization of NRG1 immunoreactivity at cholinergic synapses.

A. Maximum intensity projection of three consecutive confocal slices showing a retrogradely labeled PhrMn (blue), synapses labeled by NRG1 (green), and the vesicular acetylcholine transporter VAChT (red). Areas of co-localization that appear yellow designate the intersection between the VAChT- and NRG1-immunoreactivity. Bar: 20 μm.

B. Orthogonal projections of a single synapse (identified by an asterisk in A) showing co-localization of NRG1 and VAChT in 3D. NRG1 and VAChT partially intersect and they are clearly present at the same anatomical structure.

NIH-PA Author Manuscript

NIH-PA Author Manuscript

NIH-PA Author Manuscript

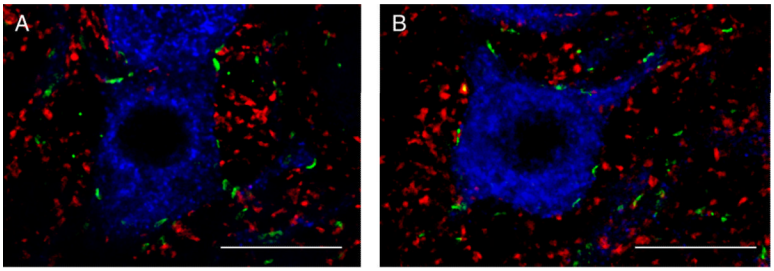

Figure 8.

Localization of NRG1 immunoreactivity at glutamatergic synapses.

A. Maximum intensity projection of two consecutive confocal slices showing a retrogradely labeled PhrMn (blue), synapses labeled by NRG1 (green), and the vesicular glutamate transporter VGLUT1 (red). There are no areas of intersection between VGLUT1- and NRG1-immunoreactivity. Bar: 20 μm.

B. Maximum intensity projection of two consecutive confocal slices showing a retrogradely labeled PhrMn (blue), synapses labeled by NRG1 (green), and VGLUT2 (red). Areas of co-localization that appear yellow designate the intersection between the VGLUT2- and NRG1-immunoreactivity. Overall, ~25% of the NRG1 immunoreactive synapses at PhrMn are associated with VGLUT2 expression. Bar: 20 μm.

NIH-PA Author Manuscript

NIH-PA Author Manuscript

NIH-PA Author Manuscript

Table 1

List of primary antibodies

Antigen	Immunogen	Manufacturer/Species	Dilution used
Cholera Toxin B	Highly purified B-subunit isolated from *Vibrio cholerae* Inaba 569B	List Biologicals (Campbell, CA) Goat polyclonal, Lot# 7023A5	1:500
NRG-1 α/β1/2	Peptide at C-terminus of the human NRG-1 isoform HRG-α (a.a. 620–640)	Santa Cruz Biotechnologies (Santa Cruz, CA) Rabbit polyclonal, sc-348, Lot# G1808	1:400
Synaptophysin	Vesicular fraction of bovine brain	Chemicon/Millipore (Billerica, MA) Mouse monoclonal MAB 5258, clone SY 38 Lot# LV1414366	1:400
VAChT	Peptide at the N-terminus of human VAChT (a.a. 1–33)	Santa Cruz Biotechnologies (Santa Cruz, CA) Goat polyclonal, sc-7717, Lot# D0307	1:100
VGLUT1	Strep-Tag fusion protein of rat VGLUT 1 (a.a. 456 – 560).	Synaptic Systems (Germany) Mouse monoclonal, clone 317D5, Lot# LV1417804	1:400
VGLUT2	Recombinant protein from rat VGLUT2	Millipore (Billerica, MA) Mouse monoclonal MAB5504, Lot# LV11616024	1:400

NRG: neuregulin; VAChT: Vesicular Acetylcholine Transporter, VGLUT: Vesicular Glutamate Transporter